Minimization of Electrical Losses in Two-Axis Tracking PV Systems

Kyriaki-Nefeli D. Malamaki and Charis S. Demoulias, *Senior Member, IEEE*

***Abstract*—In this paper, approximate analytical expressions for the power duration curve, the optimum inverter size, the annual energy losses in dc and ac cables, the annual energy losses in the step-up transformer, and the optimum transformer size have been derived for photovoltaic plants mounted on two-axis tracking systems in any European location and of any size. The derived analytical expressions contain only a few unknown parameters, which can be easily estimated from freely available climate data or data provided by the equipment (inverters or transformer) manufacturer. The analytical expressions can be a valuable tool for the design engineers for comparing–from the energetic point of view–different inverter types, cable cross sections, and transformer sizes without having to perform multiple detailed simulations, as the current practice is. The accuracy of the results obtained by the derived analytical expressions was tested against results obtained by detailed mathematical calculations. Furthermore, the model for the PDC and the expression for the annual energy losses on the three-phase cables are verified by comparison with measurements taken from a real photovoltaic installation during the past entire year.**

***Index Terms*—Cable losses, inverter size, photovoltaic plants, solar inverters, transformer losses, two-axis sun tracking systems.**

I. Introduction

PHOTOVOLTAIC (PV) systems with two-axis tracking mechanisms are employed in order to increase the annual energy yield. These systems are economically viable, because the additional cost of the tracking mechanism is paid back by the additional energy yield [1]–[11] within a reasonably short-time period especially in areas with high solar irradiation, such as the Mediterranean basin.

Since the electricity production from PV systems is still expensive, the minimization of system losses is of great importance. Significant parts of the system losses are the losses in the electrical part of the system. These losses appear in the dc and ac cables, in the dc/ac inverters and in the step-up transformers (whenever they are present).

Regarding the losses in the dc and ac cables used in a PV installation, there is not an established method for the selection of the appropriate cross-section. The common practice is to select the cross section based on the voltage drop (usually limited to 1%), which occurs when the PV system operates under standard testing conditions (STC). This practice does not take into account the fact that the loading of the cable is variable, since the PV power is also variable. In addition, it is based on cable loading, which is most unlikely to occur because a PV system rarely operates under STC.

Regarding the inverter size in PV systems, there are numerous research efforts, mainly based on simulation results, which suggest the optimum inverter size according to the geographical location, the inverter efficiency curve, and the installed PV power [12]–[20]. In [21], analytical expressions, regarding the optimum inverter size, were derived. It was shown that the optimum inverter size is a function of: 1) the maximum available electrical power at the dc terminals of the PV array and 2) the shape of the efficiency curve of the inverter. All of the aforementioned research efforts refer to PV systems with constant inclination.

Regarding the step-up transformer (whenever present), there is no established method for selecting the optimum size, from an energetic point of view. The current practice is to select the nominal power of the transformer to be equal to or slightly larger than either the installed power (under STC) of the entire PV array or the nominal power of the installed inverters. This selection, obviously, ignores that the loading of the transformer is highly variable and, therefore, the load (copper) losses of the transformer vary considerably within a year.

This paper presents an analytical method for the estimation of: 1) the power duration curve at the dc terminals of a PV system; 2) the energy produced at the ac terminals of the inverters; 3) the optimum inverter size; 4) the dc and ac cable losses; 5) the step-up transformer losses; and 6) the optimum transformer size, in PV systems mounted on two-axis tracking mechanisms in European locations. The analytical expressions concerning the optimum inverter size, the cable losses, and the transformer losses are based on an analytical expression for the duration curve of the power at the dc terminals of the PV array. Thus, contrary to the common practice and the aforementioned research, the partial loading of the ac and dc cables, the inverters, and the transformers is taken into account for the calculation of the annual energy losses on them, enabling, in this way, the selection of their size from an energetic point of view.

The shape and, thus, the analytical expression of the PDC are a function of the installed PV active power and the climate data of the particular location of the PV installation. Average climate data can be obtained freely from various sources (JRC, Meteonorm, etc). Regarding the inverter efficiency, the analytical expression, derived in [21], was used here too.

The derived analytical expressions were verified as follows: The shape of the PDC, obtained from the climate data sources, was verified in comparison with the PDC obtained by measurements in an existing two-axis tracking PV installation. The analytical expression for the annual energy losses on three-phase

Manuscript received December 21, 2012; revised April 19, 2013; accepted June 23, 2013. Date of publication July 30, 2013; date of current version September 19, 2013. Paper no. TPWRD-01392-2012.

The authors are with the Aristotle University of Thessaloniki, Thessaloniki 54621, Greece (e-mail: kyriaki_nefeli@hotmail.com; chdimoul@auth.gr).

Color versions of one or more of the figures in this paper are available online at http://ieeexplore.ieee.org.

Digital Object Identifier 10.1109/TPWRD.2013.2272405

cables was also verified by measurements in the same two-axis tracking PV installation. In general, the validity of the derived analytical expressions is verified through comparison with detailed mathematical calculations, based on the PDC obtained directly from the climate data source.

Using the derived analytical expressions, the design engineers can now compare various inverter types from the overall energy-efficiency point of view. They can also compare various cable cross-sections, taking into account the annual energy losses on them and their cost. Finally, they can compare various transformer sizes and their class of losses, based on the annual energy losses and the transformer cost. These days, in order to obtain similar results, one has to perform multiple detailed simulations.

II. Power Duration Curve of Two-Axis Tracking PV Systems

The power at the dc terminals of a PV system is a function of its nominal power under STC, the solar irradiance on the PV plane, and the PV cell temperature. Average values with a resolution of 15 min are available for every European location in [22].

It is well known that the electric power at the dc terminals of a PV array is directly proportional to the global solar irradiance on the array and varies linearly with the solar cell temperature [23]. Thus, the electric power at the dc terminals of any PV array can be expressed as

$$P_{\rm dc}(t) = P_{\rm PV,peak}\frac{G(t)}{G_{\rm STC}}[1 + DP \cdot \Delta\theta] \qquad (1)$$

where $P_{\rm dc}(t)$ is the available dc power at time t, $P_{\rm PV,peak}$ is the installed peak power under STC, $G(t)$ $(\rm W/m^2)$ is the global solar irradiance on the PV plane at time t in, and $G_{\rm STC} = 1000\ \rm W/m^2$ is the solar irradiance under STC. DP is a coefficient that expresses the power reduction due to the temperature rise in cells. A typical value for crystalline silicon cells is $DP = -0.5\%/^\circ\rm C$ [23]. $\Delta\theta$ $(^\circ\rm C)$ is the rise of the cell temperature above 25 °C.

The rise of the cell temperature above the ambient one depends on the solar irradiance, the wind velocity, and the construction details of the PV panel. Usually, the temperature increase is in the range of 22–37 °C with a mean value being 30 °C [23], [24]. Thus, $\Delta\theta$ can be calculated from

$$\Delta\theta = T_{\rm amb} + 30 - 25 \qquad (2)$$

where $T_{\rm amb}$ is the ambient temperature.

Fig. 1 shows the dc electric power available at the terminals of a PV system with $P_{\rm PV,peak} = 100\ \rm kW_p$ mounted on two-axis tracking mechanisms in Iraklion, Greece, for typical days of June and December. Similar curves can be plotted for every location and for every day of a typical year. Using these power values (i.e. the dc power averaged over 15 min), the PDC can be constructed for every European location for given PV installed power. The PDC is defined as the curve that shows the aggregate time in a year for which the dc power is larger than or equal to a certain value.

Fig. 2 shows the PDC of a 100-$\rm kW_p$ PV installation mounted on two-axis tracking mechanisms in five European locations.

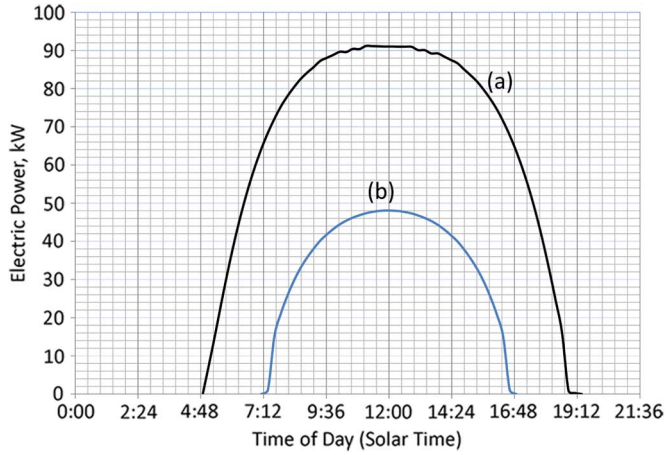

Fig. 1. Calculated electric power at the dc terminals of a 100-$\rm kW_p$ PV system mounted on two-axis tracking mechanisms for a typical day in (a) June and (b) December. Location: Iraklion, Greece.

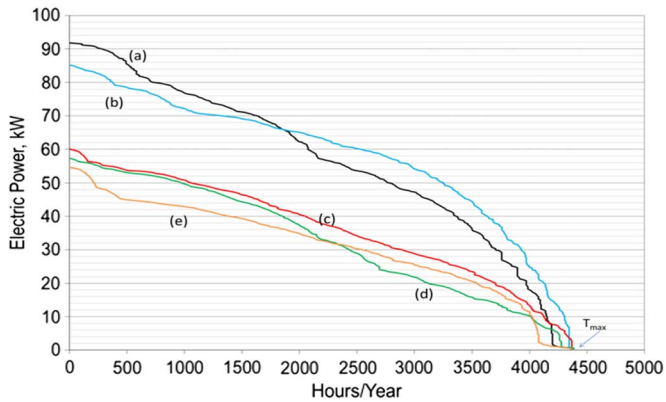

Fig. 2. Power duration curves of 100 $\rm kW_p$, two-axis-tracking PV installation in five locations: (a) Iraklion, Greece $35^\circ 19'\rm N$. (b) Madrid, Spain $40^\circ 20'\rm N$. (c) Munich, Germany $48^\circ 04'\rm N$. (d) Warsaw, Poland $52^\circ 10'\rm N$. (e) Edinburgh, U.K. $55^\circ 53'\rm N$.

The PDCs were constructed (with a resolution of 0.3 kW) by implementing (1) and (2) in a common spreadsheet software. The required average values of the solar irradiance and ambient temperature were extracted from [22] for the specific locations. It should be noted that in order to avoid the effect of microclima present within large cities, the locations mentioned in Fig. 2 do not correspond to the centers of the respective cities but to the outskirts of them. Every PDC has two characteristic values: the maximum power $P_{\rm max}$ at $t = 0$ and the maximum annual duration $T_{\rm max}$ at which $P_{\rm max} = 0$.

It can be noticed from Fig. 2 that as we move southwards, the maximum electrical power $P_{\rm max}$ increases while the maximum annual duration $T_{\rm max}$ of all the PDC curves is almost the same, since it is the daytime in a year and, therefore, approximately equal to half the total number of hours per year, that is, 4400 h. The actual value of $T_{\rm max}$ is 4385, 4392, 4408, 4415, and 4423 h for Iraklion, Madrid, Munich, Warsaw, and Edinburgh, respectively. $T_{\rm max}$ appears in all subsequent expressions related to the energy losses in the cables, in the inverters, and in the transformers. If we assume $T_{\rm max}$ constant for every location and equal to 4400 h, we will introduce an error of less than $(4423-4400)/4400 = 0.0052$ or 0.52% for the locations under

TABLE I
ERRORS IN THE ESTIMATION OF PDCS

	Energy content from actual PDC, MWh/year	Energy content from PDC with (3), MWh/year	Error in energy estimation, %	R_{xy}
Iraklion	248	252	1.80	0.994
Madrid	256	266	3.72	0.996
Munich	160	164	2.36	0.997
Warsaw	144	145	0.87	0.994
Edinburgh	137	141	3.06	0.989

consideration. If more accuracy is required, then the actual value of $T_{\max}$ for a specific location must be calculated by building the actual PDC.

After numerous efforts with MATLAB, it was found that the function that best fits the PDCs shown in Fig. 2 (as well as the PDC in other European locations) has the form

$$P(t) = \frac{A + t}{B + C \cdot t}. \tag{3}$$

Parameters A, B, and C in (3) are specific for each location and can be calculated—using MATLAB or another software—after the PDC has been built. The challenge is to estimate these parameters from others that are readily available without having to build the PDC.

It was previously discussed that assuming $T_{\max} = 4400$ h for each location does not introduce significant error. Thus, for every PDC, $P(t = 4400) = 0$, which gives

$$A = -T_{\max} = -4400. \tag{4}$$

Since $P(0) = P_{\max}$, we have

$$P_{\max} = \frac{A}{B} \Rightarrow B = \frac{A}{P_{\max}}. \tag{5}$$

Now that the parameters A and B are known in terms of $P_{\max}$ and $T_{\max}$, parameter C can be calculated from (3), if $P(\mathrm{t})$ is known for some $0 < t < T_{\max}$, which assumes that the respective PDC is known. Using (3)–(5), the values of parameter C that give the best fit were calculated for 18 European locations ranging from Iraklion, Greece, in the south to Edinburgh, U.K., in the north and from Madrid, Spain, in the west to Warsaw, Poland, in the east. Correlating the values of C to those of $P_{\max}$, A and B, it was found that a good guess for C is the following:

$$C = \frac{A + 1000}{867.5 \cdot P_{\max}} - \frac{B}{1000} \tag{6}$$

which, by using (4) and (5), gives

$$C = \frac{0.481}{P_{\max}}. \tag{7}$$

Adopting a more "elegant" expression

$$C = \frac{1}{2 \cdot P_{\max}} \tag{8}$$

the additional introduced error is insignificant, as shown in Table I and subsequently. Fig. 3 shows, for two different European locations, the PDC obtained with (3) and the PDC built using climate data in (1) and (2).

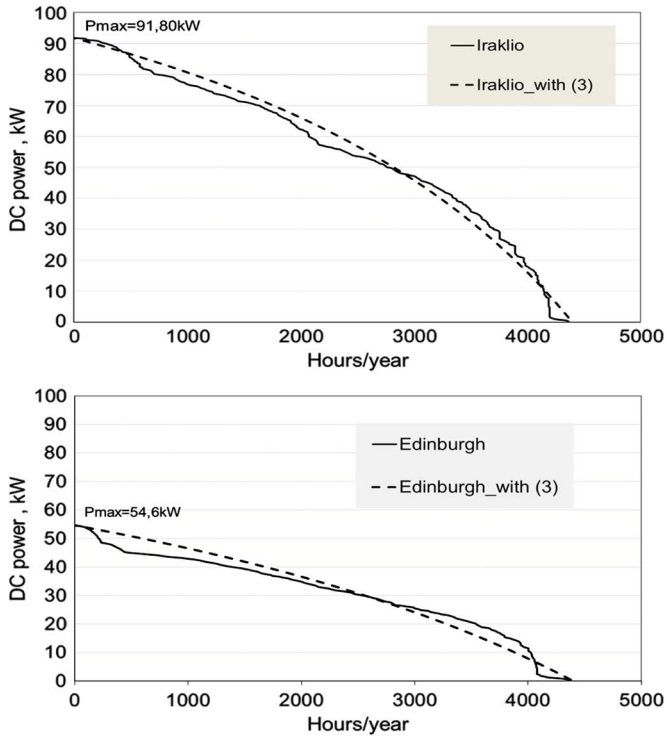

Fig. 3. Comparison between the actual PDC and the PDC calculated by (3) in two locations.

Two metrics are used to estimate the error introduced when using (3) instead of the actual PDC. The actual PDC can be either calculated from climate data using (1) and (2) or built from available measurements. The first metric is the energy content of the installation, which is equal to the area beneath the PDC. The second metric is the correlation coefficient R_{xy} among the two curves. Table I shows both metrics for five locations for an installed PV power of 100 $\mathrm{kW_p}$. We observe that the maximum error in the estimation of the energy content is 3.72%, while the minimum R_{xy} is 0.989. It can be found that for 50 $\mathrm{kW_p}$, the respective values are 3.5% and 0.989, while for 200 $\mathrm{kW_p}$, they are 4% and 0.990, respectively. Thus, using (3)–(5) and (8) for the estimation of the PDC does not introduce significant error, while the error itself is not sensitive to the magnitude of the installed power.

It is evident from (3)–(5) and (8) that the only parameter needed in order to define the PDC is $P_{\max}$. The latter can be easily estimated by searching a few combinations of large irradiance and relatively low ambient temperature in any climate database, using (1) and (2). Such combinations usually appear in the period from May to July for northern hemisphere locations. Therefore, it is not necessary to build the PDC in order to find $P_{\max}$.

The validity of the proposed method for the calculation of the PDC using only $P_{\max}$, is demonstrated in Fig. 4, where the calculated PDC of an existing PV installation of 80 $\mathrm{kW_p}$ in the island of Crete, Greece $(35°03'\mathrm{N}, 24°59'\mathrm{E})$ is compared to the PDC that was built from actual measurements that correspond to the period from April 1, 2011 to March 31, 2012.

It can be observed that: 1) The PDC calculated using (1) and (2), and average climate data from [22] has the same shape as

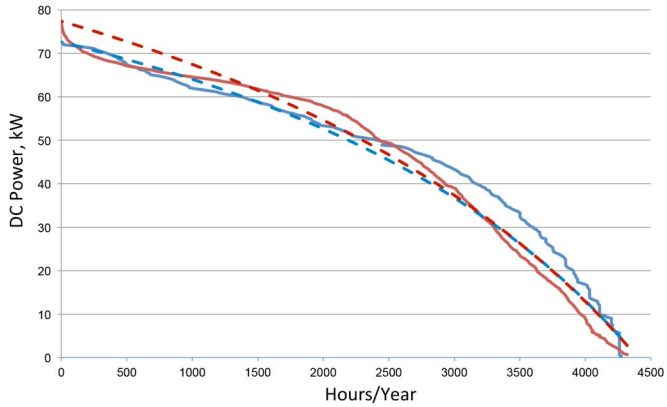

Fig. 4. Power duration curves of 80 kWp, two-axis-tracking PV installation in Crete, Greece, location $35^{\circ}19'\mathrm{N}$; Blue solid line: PDC obtained from statistical data available in [22]; Red solid line: PDC built from measurements; Dashed lines: respective PDCs calculated from (3).

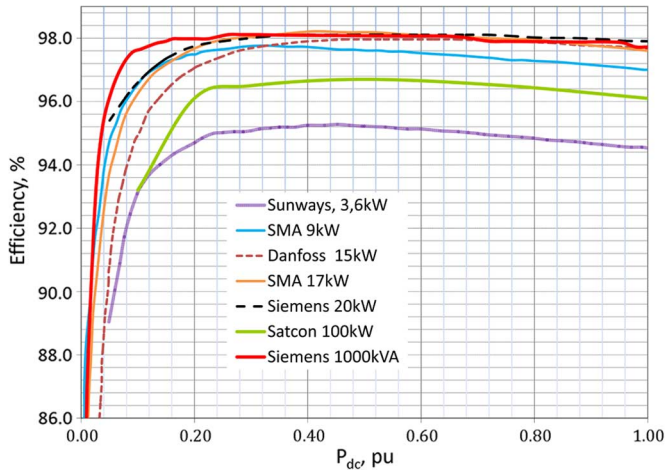

Fig. 5. Efficiency curve of various solar inverters.

the PDC obtained from measurements. Of course, the value of $P_{\max}$ is different (77.37 kW measured and 72.6 kW estimated from [22]) and 2) the PDCs that are estimated using (3) for the respective $P_{\max}$ (shown in dashed lines) approximate with sufficient accuracy the original PDCs, since the correlation factors are 0.989 and 0.992, while the energy errors are 4.16% and 2.46% for the calculated and measured case, respectively.

III. Analytical Expressions for the Ac Energy Yield and the Optimum Inverter Size

The efficiency η of a solar inverter is defined by

$$\eta(t) = \frac{P_{\mathrm{ac}}(t)}{P_{\mathrm{dc}}(t)} = \frac{P_{\mathrm{dc}}(t) - P_{loss}(t)}{P_{\mathrm{dc}}(t)} \tag{9}$$

where $P_{\mathrm{dc}}(\mathrm{t})$, $P_{\mathrm{ac}}(\mathrm{t})$, and $P_{\mathrm{loss}}(\mathrm{t})$ are the instantaneous dc power, ac power, and power loss, respectively.

The efficiency of a solar inverter is not constant, but it depends on the loading of the inverter. This fact can be seen in the shape of the efficiency curve versus the per-unit (p.u.) dc power of various inverters shown in Fig. 5. The curves were extracted from the technical brochures of the respective inverter manufacturers. The nominal power of the inverters is in the range of 3.6–1000 kW. It can be noticed from Fig. 5 that the efficiency of all inverters drops abruptly at power levels below 0.2 p.u. This means that an inverter, which is largely oversized with respect to the PV power, will operate for longer periods (during sunrise, sunset or in cloudy days) with reduced efficiency. On the other hand, an inverter with relatively small rated power will not transfer the dc power that is larger than its rated power to the ac grid, since an inverter does not allow its ac current to exceed its nominal value. It is, thus, evident, that for a given PV installation (i.e., given PDC) and inverter type (i.e., given the shape of the efficiency curve), there is an optimum inverter size, which will result in maximization of the inverter efficiency over the entire operating range.

It is also evident from Fig. 5 that the maximum efficiency of an inverter is achieved only within a small operating range of its rated power. Thus, for the evaluation of an inverter, its efficiency over the entire operating range and not just its maximum efficiency value should be considered. This is the reason for the establishment of the Euro-efficiency value, which is a dynamic efficiency, weighted for the Central European climate [25]. The Euro efficiency η_{Euro} is defined by

$$\eta_{\mathrm{Euro}} = 0.03 \cdot \eta_{5\%} + 0.06 \cdot \eta_{10\%} + 0.13 \cdot \eta_{20\%} + 0.10 \cdot \eta_{30\%} + 0.48 \cdot \eta_{50\%} + 0.2 \cdot \eta_{100\%} \tag{10}$$

where it is assumed that the inverter will operate at its nominal power only for 20% of its operating time over a year, at 50% of its nominal power for 48% of its operating time over a year, and so on. Thus, the time coefficients in (10) represent average values, which correspond to the Central European climate conditions, and average inverter efficiency curves during 1991, the time where Euro-efficiency was introduced. Additionally, Euro-efficiency was established having in mind only PV systems with fixed inclination. It is obvious from Fig. 3 that a given inverter will operate, at a given power level, for different time periods depending on the location. For this reason, the Euro-efficiency cannot generally represent the effective inverter efficiency over its whole operating range. This assertion will be proved later.

The efficiency curve of any solar inverter can be described, with very good accuracy, by [21]

$$\eta(P_{\mathrm{dc,p.u.}}) = D + G \cdot P_{\mathrm{dc,p.u.}} + \frac{F}{P_{\mathrm{dc,p.u.}}} \tag{11}$$

where η is the efficiency of the inverter in percent, $P_{\mathrm{dc,p.u.}} > 0$ is the per-unit value of the dc power, while D, G, and F are parameters that can be easily determined from the efficiency curve of the specific inverter by taking three (η, $P_{\mathrm{dc,p.u.}}$) pairs and solving a system of three linear equations. The pairs that correspond to $P_{\mathrm{dc,p.u.}} = 0.1$, 0.2 and 1 p.u. are very good choices, because (as shown in Fig. 5) $P_{\mathrm{dc,p.u.}} = 0.1$ p.u. corresponds to the rising front of the efficiency curve, $P_{\mathrm{dc,p.u.}} = 0.2$ p.u. corresponds to a region near the "peak" of the curve and $P_{\mathrm{dc,p.u.}} =$ 1 p.u. corresponds to the "tail" of the curve.

Table II shows the values of the D, G, and F parameters of the inverters shown in Fig. 5 along with the correlation coefficient R_{xy} between the actual efficiency values and the ones estimated by (11), where the very good accuracy of (11) is obvious.

TABLE II
D, G, AND F PARAMETERS USED IN (11) FOR VARIOUS INVERTERS. R_{xy} IS THE CORRELATION COEFFICIENT

	D	G	F	R_{xy}
Sunways, 3.6kW	96.83	-1.95	-0.347	0.997
SMA, 9kW	98.93	-1.70	-0.221	0.986
Danfoss, 15kW	99.69	-1.56	-0.464	1.000
SMA, 17kW	99.63	-1.70	-0.325	0.986
Siemens, 20kW	99.22	-1.08	-0.252	0.982
Satcon, 100kW	99.97	-3.22	-0.644	0.995
Siemens, 1000kW	98.57	-0.76	-0.088	0.993

Since the PDC and the inverter efficiency are known functions of time, the annual energy yield $E_{\rm ac}$ at the ac side of the inverters can be estimated. Then, the optimum—from an energetic point of view—inverter size of a given PV installation can be calculated. The annual energy that will be injected into the ac grid can be calculated with the aid of (3) and (11) for two distinctive cases. In the first case, it is assumed that $P_{\rm inv,N} \geq P_{\rm max}$, while in the second case, $P_{\rm inv,N} \leq P_{\rm max}$, where $P_{\rm inv,N}$ is the nominal power of all the inverters in a PV installation

If $P_{\rm inv,N} \geq P_{\rm max}$, the annual energy yield $E_{\rm ac}$ is given by

$$E_{\rm ac} = \int_0^{T_{\rm max}} P_{\rm dc}(t) \cdot \eta(P_{\rm dc,p.u.}) \cdot dt = \int_0^{T_{\rm max}} P_{\rm dc}(t)\left(D + G\frac{P_{\rm dc}(t)}{P_{\rm inv,N}} + F\frac{P_{\rm inv,N}}{P_{\rm dc}(t)}\right) \cdot dt \quad (12)$$

$P_{\rm dc}(t)$ is given by (3), while the D, G, and F parameters must be in decimal form (i.e., not in percentage as shown in Table II). It is obvious from (12) that since $P_{\rm inv,N} \geq P_{\rm max}$, the inverter never operates in power-limitation mode.

Using (3)–(5) and (8), (12) gives

$$E_{\rm ac} = T_{\rm max} \cdot \left\{ F \cdot P_{\rm inv,N} + 2 \cdot D \cdot P_{\rm max} \cdot [1 - \ln(2)] + \frac{2 \cdot G \cdot P_{\rm max}^2}{P_{\rm inv,N}} \cdot [3 - 4\ln(2)] \right\}. \quad (13)$$

The optimum, from the energetic point of view, inverter size is the one that maximizes $E_{\rm ac}$. It can be found from

$$\frac{dE_{\rm ac}}{dP_{\rm inv,N}} = 0 \Rightarrow P_{\rm inv,N}^{\rm opt} = P_{\rm max}\sqrt{\frac{2 \cdot G \cdot [3 - 4 \cdot \ln(2)]}{F}}. \quad (14)$$

Substituting (14) in (13), the maximum energy yield at the ac side (for a given location, installed PV power, and inverter type) can be calculated.

If $P_{\rm inv,N} \leq P_{\rm max}$, the inverter will operate normally for $T_{\rm max} - T_{\rm inv,N}$ h/yr, but for $T_{\rm inv,N}$ h/yr, it will deteriorate the injected power to its nominal power. The annual energy yield is given by

$$E_{\rm ac} = T_{{\rm inv},N} \cdot P_{{\rm inv},N} \cdot \eta(P_{\rm inv,N,p.u.}) + \int_{T_{{\rm inv},N}}^{T_{\rm max}} P_{\rm dc}(t) \cdot \eta(P_{\rm dc,p.u.}) \cdot dt. \quad (15)$$

TABLE III
OPTIMUM INVERTER SIZE IN KILOWATTS CALCULATED WITH (14). SHADED CELLS: ACCURATE CALCULATIONS BASED ON THE ACTUAL PDC AND ACTUAL INVERTER EFFICIENCY CURVE. (100 kWp INSTALLATION)

Efficiency curve like:	Iraklion	Madrid	Munich	Warsaw	Edinburgh
Sunways, 3.6kW	147	136	96	92	87
	146	142	94	89	84
SMA, 9kW	172	159	113	107	102
	171	166	110	102	98
Danfoss, 15kW	114	105	75	71	68
	113	110	73	69	66
SMA, 17kW	142	131	93	88	84
	141	136	91	85	81
Siemens, 20kW	128	119	84	80	76
	128	124	82	77	74
Satcon, 100kW	138	128	91	86	82
	138	133	89	83	80
Siemens, 1000kW	182	169	120	114	108
	182	173	116	109	105

From (11), the inverter efficiency at nominal power is

$$\eta(P_{\rm inv,N,p.u.}) = D + G + F. \quad (16)$$

$T_{\rm inv,N}$ is the time where $P_{\rm inv,N} = P_{\rm dc}(T_{\rm inv,N})$ and it can be calculated from (3)

$$P_{\rm inv,N} = \frac{A + T_{\rm inv,N}}{B + C \cdot T_{\rm inv,N}} \Rightarrow T_{\rm inv,N} = \frac{A \cdot C \cdot P_{\rm inv,N}}{1 - C \cdot P_{\rm inv,N}} - A. \quad (17)$$

Using (3)–(5), (8), and (15)–(17)

$$E_{\rm ac} = T_{\rm max} \cdot \left\{ 2 \cdot P_{\rm max} \cdot \ln\left(1 - \frac{P_{inv,N}}{2 \cdot P_{\rm max}}\right) \cdot \left[D + \frac{4 \cdot G \cdot P_{\rm max}}{P_{\rm inv,N}}\right] + 4 \cdot G \cdot P_{\rm max} + P_{\rm inv,N} \cdot (F + 2 \cdot D + 2 \cdot G) \right\}. \quad (18)$$

It is obvious from (18) that the derivative $dE_{\rm ac}/dP_{\rm inv,N}$ will contain, apart from $P_{\rm inv,N}$, the term $\ln[1 - P_{\rm inv,N}/(2 \cdot P_{\rm max})]$. Hence, an analytical expression for $P_{\rm inv,N}$ cannot be derived. However, solving numerically this derivative, it was found that the optimum inverter size is $P_{\rm inv,N} = P_{\rm max}$ for a wide range of inverters that were examined. The optimum inverter size can be smaller than $P_{\rm max}$ in the hypothetical case where $|F| \geq |G|$. Nevertheless, there are no such, at least commercially available, inverters.

The most accurate calculation of the optimum inverter size can be made by using the actual PDC (Fig. 2) and the actual inverter efficiency curve (Fig. 5) given by the inverter manufacturer. Table III shows in comparison the optimum inverter size calculated according to the aforementioned accurate method and according to (14) for various locations and inverter types, i.e. inverters with the specific efficiency curves, assuming 100 $\rm kW_p$ PV installation.

It is evident from Table III that (14) can be used for calculating the optimum inverter size in two-axis tracking PV systems with very good accuracy. Since the values in Table III correspond to 100 $\rm kW_p$ PV installation, they can also be read as percentages of the nominal installed PV power. It is clear from Table III that the shape of the efficiency curve of the inverter has

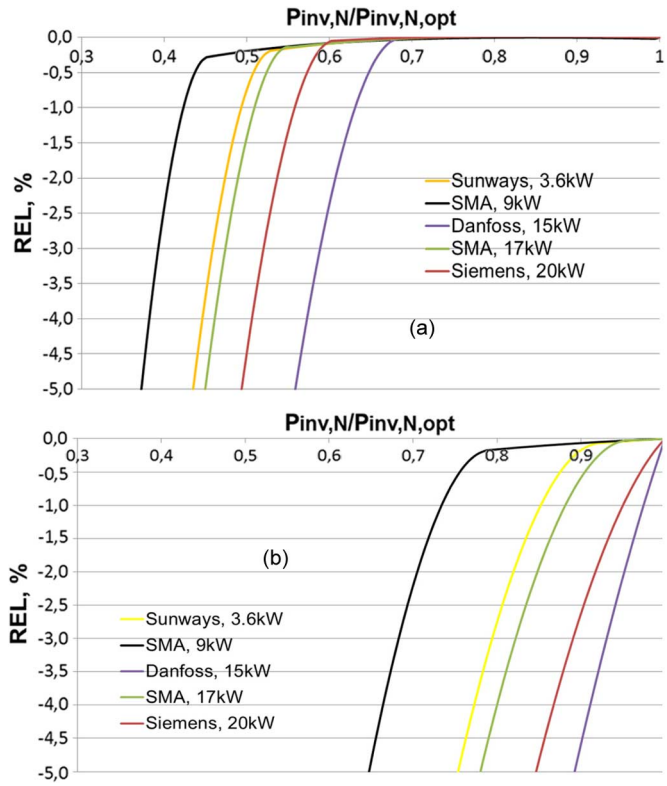

Fig. 6. REL as a function of inverter type and relative inverter size with respect to the optimum one for (a) Iraklion, Greece and (b) Edinburgh, U.K.

a significant impact to its optimum size in a given location. For example, in Iraklion, which is the southernmost location examined, the optimum inverter size varies in the range 114–182 kW, while in Edinburgh, which is the northernmost location examined, the optimum inverter size, is in the range 68–105 kW.

If an inverter with size other than the optimum is selected, the produced ac energy $E_{\rm ac}$ will be smaller than the maximum $E_{\rm ac,max}$. Let us define, the relative ac energy loss (REL) as

$$\mathrm{REL} = \frac{E_{\rm ac,max} - E_{\rm ac}}{E_{\rm ac,max}} 100. \tag{19}$$

Fig. 6 shows the REL when selecting inverter sizes in the range 0.3–1.0 p.u. with the optimum inverter size selected as the per-unit basis. Since the curves shown in Fig. 6 are normalized, they are independent of the installed PV power. The REL in Fig. 6 was calculated for the southernmost (Iraklion) and the northernmost (Edinburgh) PV installations examined.

It is clear from Fig. 6 that the sensitivity of the ac energy production depends on the shape of the inverter efficiency curve and the geographical location of the PV installation. The sensitivity of the REL with respect to the optimum inverter size is relatively small in southern locations, while in northern locations, the sensitivity is much larger. The curves in Fig. 6 can be read in two ways: 1) one can determine the REL when selecting an inverter size that is a percentage of the optimum one and 2) for a predetermined REL, one can the select the relative inverter size (with respect to its optimum one) for a given shape of the efficiency curve.

TABLE IV
EFFICIENCY VALUES OF VARIOUS INVERTERS

Inverter Types:	$\eta_{\rm eff,opt}$ $P_{\rm inv,N}>P_{\rm max}$	$\eta_{\rm eff,opt}$ $P_{\rm inv,N}=P_{\rm max}$	$\eta_{\rm max}$	$\eta_{\rm Euro}$
Sunways, 3.6kW	0,950	0,948	0,953	0,947
SMA, 9kW	0,976	0,973	0,980	0,976
Danfoss, 15kW	0,978	0,978	0,980	0,974
SMA, 17kW	0,980	0,978	0,982	0,978
Siemens, 20kW	0,981	0,980	0,982	0,978
Satcon, 100kW	0,966	0,965	0,967	0,960
Siemens, 1000kW	0,980	0,979	0,981	0,979

If the optimum inverter size is selected, we can define the effective overall inverter efficiency as

$$\eta_{\rm eff,opt} = \frac{E_{\rm ac,max}}{E_{\rm dc}} = \frac{E_{\rm ac,max}}{\int_0^{T_{\rm max}} P_{\rm dc}(t)dt} \tag{20}$$

where $P_{\rm dc}(t)$ is given by (3) and $E_{\rm ac,max}$ can be calculated by (13) using the optimum inverter size calculated by (14), if $P_{\rm inv,N} > P_{\rm max}$ or by (18) if $P_{\rm inv,N} = P_{\rm max}$. Equation (20) gives

$$\eta_{\rm eff,opt} = \frac{E_{\rm ac,max}}{E_{\rm dc}} = D - \frac{\sqrt{2\cdot F\cdot G\cdot(3-4\cdot\ln 2)}}{(1-\ln 2)} \tag{21}$$

for $P_{\rm inv,N} > P_{\rm max}$ and

$$\eta_{\rm eff,opt} = \frac{E_{\rm ac,max}}{E_{\rm dc}} = D + \frac{F + 2\cdot G\cdot(3-4\cdot\ln 2)}{2\cdot(1-\ln 2)} \tag{22}$$

for $P_{\rm inv,N} = P_{\rm max}$.

As can be seen from (21) and (22), the effective inverter efficiency is independent of the location, since the selected optimum inverter size is location-dependent.

Table IV shows the maximum inverter efficiency, the Euro-efficiency, and the effective overall inverter efficiency for the various inverters examined. It is evident from Table IV that the effective overall inverter efficiency (when the optimum inverter size is selected) is, in all cases, larger than the Euro-efficiency and smaller than the maximum one.

IV. ENERGY LOSSES IN THE DC AND AC CABLES

Since the PDC of any two-axis tracking PV system can be expressed analytically with (3), it is possible to derive an analytical expression for the annual energy losses in the cables of such PV installation. The calculation of the annual cable energy losses (instead of just the power losses under STC, which is the current practice) along with the cable cost can be a valuable tool to the design engineer in selecting the appropriate cable cross-section, based on technical and economic criteria.

In a PV installation, dc cables are used for the connection of the PV strings with the inverter. We will assume that $N_{\rm t}$ is the total number of strings in a PV installation and N the number of strings that are connected to an individual dc cable. The power losses in that cable at time t, is given by

$$\begin{aligned} P_{\rm dc\_cbl,loss}(t) &= 2\cdot I^2_{\rm dc,cable}(t)\cdot r_{\rm dc} \\ &= 2\cdot\left(\frac{P_{\rm dc,cable}(t)}{V_{\rm dc}}\right)^2\cdot r_{\rm dc} = \frac{2\cdot r_{\rm dc}}{V^2_{\rm dc}} P^2_{\rm dc,cable}(t) \\ &= \frac{2\cdot r_{\rm dc}}{V^2_{\rm dc}}\left(\frac{N}{N_t}\right)^2 P^2_{\rm dc}(t) \end{aligned} \tag{23}$$

where $r_{\rm dc}$ is the resistance of the dc cable, while $V_{\rm dc}$ is the dc voltage at the cable terminals (this is actually the MPP dc voltage applied by the inverter) and is considered constant. It actually varies with the solar radiation and temperature conditions, but its variation is within ±10% of its design value.

If $P_{\rm inv,N} \geq P_{\rm max}$, $P_{\rm dc}(t)$ is given by (3) and taking into account (4), (5) and (8), we define

$$W_1 = \int_0^{T_{\rm max}} P_{\rm dc}^2(t)dt = \int_0^{T_{\rm max}} \left(\frac{A+t}{B+C\cdot t}\right)^2 dt = 2\cdot T_{\rm max}\cdot P_{\rm max}^2\cdot[3-4\ln(2)]. \quad (24)$$

In case $P_{\rm inv,N} \leq P_{\rm max}$, $P_{\rm dc}(t)$ is given by (3) from $t = T_{\rm inv,N}$ to $t = T_{\rm max}$, whereas $P_{\rm dc}(t) = P_{\rm inv,N}$ from $t = 0$ to $t = T_{\rm inv,N}$. We define

$$W_2 = \int_0^{T_{\rm inv,N}} P_{inv,N}^2 dt + \int_{T_{\rm inv,N}}^{T_{\rm max}} \left(\frac{A+t}{B+C\cdot t}\right)^2 dt = 8\cdot T_{\rm max}\cdot P_{\rm max}^2\cdot\left[\ln\left(1-\frac{P_{inv,N}}{2\cdot P_{\rm max}}\right)+\frac{P_{\rm inv,N}}{2\cdot P_{\rm max}}\cdot\left(1+\frac{P_{\rm inv,N}}{2\cdot P_{\rm max}}\right)\right]. \quad (25)$$

There is no physical meaning in W_1 and W_2. The main reason they were derived is to make the subsequent expressions of the cable and the transformer losses simpler.

If $P_{\rm max}$ is expressed in watts, the energy losses will be in Wh.

If $P_{\rm inv,N} \geq P_{\rm max}$,the annual energy losses in a dc cable can be calculated by using (23) and (24) from

$$E_{\rm dc\_cbl,loss} = \int_0^{T_{\rm max}} P_{\rm dc\_cbl,loss}(t)dt = \frac{2\cdot r_{\rm dc}}{V_{\rm dc}^2}\cdot\left(\frac{N}{N_t}\right)^2\cdot W_1. \quad (26)$$

In case $P_{\rm inv,N} \leq P_{\rm max}$, using (23) and (25)

$$E_{\rm dc\_cbl,loss} = \int_0^{T_{\rm inv,N}} P_{\rm dc\_cbl,loss}(t)dt + \int_{T_{\rm inv,N}}^{T_{\rm max}} P_{\rm dc\_cbl,loss}(t)dt = \frac{2\cdot r_{\rm dc}}{V_{\rm dc}^2}\cdot\left(\frac{N}{N_t}\right)^2\cdot W_2. \quad (27)$$

The ac cables are used for the connection of the inverter with an ac switchboard, either main or secondary. We will assume that $N_{\rm it}$ is the total number of inverters in a PV installation and N_i is the number of the inverters that are connected to an individual ac cable.

In order to derive an equally simple expression for the annual energy losses in the ac cables, we will ignore the losses on the inverters and assume that $P_{\rm ac}(t) = P_{\rm dc}(t)$. This simplification inevitably introduces an error, if the absolute value of the cable losses is to be calculated. However, such a simplification can be justified, because: (1) the effective annual efficiency of the inverters is very high (larger than 97%) and (2) for the selection of the appropriate cable cross-section, we are mainly interested in comparing the annual energy losses among different cable cross-sections, rather than calculating their absolute values.

With single-phase inverters, the annual energy losses in the ac cables are given by expressions similar to (26) and (27), respectively. In case that $P_{\rm inv,N} \geq P_{\rm max}$,

$$E_{\rm ac\_cbl,loss}^{1ph} = \frac{2\cdot r_{\rm ac}}{V_{1ph}^2}\cdot\left(\frac{N_i}{N_{\rm it}}\right)^2\cdot W_1 \quad (28)$$

where $r_{\rm ac}$, is the resistance of the ac cable in the fundamental frequency, $V_{1\rm ph}$ is the line-to-neutral voltage at the ac terminals of the inverter. If $P_{\rm inv,N} \geq P_{\rm max}$,

$$E_{\rm ac\_cbl,loss}^{1ph} = \frac{2\cdot r_{\rm ac}}{V_{1ph}^2}\cdot\left(\frac{N_i}{N_{\rm it}}\right)^2\cdot W_2. \quad (29)$$

With three-phase inverters, the power losses in an ac cable are

$$P_{\rm ac\_cable,loss}(t) = 3\cdot I_{\rm ac,cable}^2(t)\cdot r_{\rm ac} = 3\cdot\left(\frac{P_{\rm dc,cable}(t)}{\sqrt{3}\cdot V_{LL}}\right)^2\cdot r_{\rm ac} = \frac{r_{\rm ac}}{V_{LL}^2}\cdot\left(\frac{N_i}{N_{\rm it}}\cdot P_{\rm dc}(t)\right)^2 = \frac{r_{\rm ac}}{V_{LL}^2}\cdot\left(\frac{N_i}{N_{it}}\right)^2\cdot P_{\rm dc}^2(t) \quad (30)$$

where $I_{\rm ac,cable}$ is the rms value of the line current and V_{LL} is the rms value of the line voltage at the ac side. It is assumed that: 1) the inverter operates at unity power factor (as the case in almost all installations, until now, is) and 2) $V_{\rm LL}$ is constant.

If $P_{\rm inv,N} \geq P_{\rm max}$, the annual energy losses in the three-phase cable can be calculated by using (23) and (30),

$$E_{\rm ac\_cbl,loss}^{3ph} = \int_0^{T_{\rm max}} P_{\rm ac\_cbl,loss}(t)dt = \frac{r_{\rm ac}}{V_{LL}^2}\cdot\left(\frac{N_i}{N_{it}}\right)^2\cdot W_1 \quad (31)$$

while if $P_{\rm inv,N} \leq P_{\rm max}$, the annual energy losses in the three-phase cable can be calculated by using (25) and (30)

$$E_{\rm ac\_cbl,loss}^{3ph} = \int_0^{T_{\rm inv,N}} P_{\rm ac\_cbl,loss}(t)dt + \int_{T_{\rm inv,N}}^{T_{\rm max}} P_{\rm ac\_cbl,loss}(t)dt = \frac{r_{\rm ac}}{V_{LL}^2}\cdot\left(\frac{N_i}{N_{\rm it}}\right)^2\cdot W_2. \quad (32)$$

The validity of (31) has been tested against measurements taken in the real 80 $\rm kW_p$ PV installation mentioned in Section II. In this installation, nine single-phase SMA 9-kW inverters were used. Every three single-phase inverters were combined in a three-phased system. Each three-phase system was connected to the main switchboard via a $\rm J1VV4\times10\ mm^2$ cable. The length of the cable of each system was 120 m, 60 m and 25 m, respectively. The cables run in plastic pipes in the ground for most of their part. The actual conductor temperature varies according to the ambient temperature and the cable loading and it is not monitored. The annual energy losses in each ac cable were calculated using (31) and were found to be 1.827, 0.913, and 0.38 MWh, respectively. In total, the annual energy losses in the ac cables are 3.12 MWh. The detailed

TABLE V
CONFIGURATION OF EACH THREE-PHASE SYSTEM IN THE 80 kW_p INSTALLATION

Inverter Type	SMA 9kW
$P_{inv,N}$	3x9=27kW
AC cable type	J1VV4x10mm^2
R_{ac} (mΩ/m) at 20°C	1.83
N_i	1
N_{it}	3
V_{LL} (V)	400
T_{max} (h)	4400
P_{max} (W)	77370
W_1	$1.198 \cdot 10^{13}$

parameters for the calculation of the ac cable losses are shown in Table V.

The PV installation has a monitoring system, which records a large number of electrical and climate parameters, including the energy produced at the ac terminals of each inverter. For the time period from 01/04/2011 to 31/3/2012 the monitoring system recorded 185.467 MWh. The energy meter of the Distribution Network Operator recorded 182.311 MWh. The only losses that appear between the ac terminals of the inverters and the energy meter are the ac cable losses (there is no step-up transformer since the installed power of this plant is below 100 kW_p). Therefore, the measured annual energy losses in the ac cables of the installation are $185.467 - 182.311 = 3.156$ MWh. Thus, the error between the calculated and measured energy losses is $(3.156 - 3.12)/3.156 = 0.0114$ or 1.14%. This error can be justified by the fact that we assumed the conductor temperature to be 20 °C (as shown in Table V),while the actual conductor temperature is not known. It is obvious that (31) can accurately calculate the annual energy losses along three-phase cables, provided that P_{max} and the rest of the parameters shown in Table V are known.

The measured energy losses in the ac cables correspond to $3.156/185.467 = 0.017$ or 1.7% of the energy produced at the output of the inverters. If the actual P_{max} were not known, we would use the estimated one, which is 72.6 kW, as shown in Section II. In this case, using (13), the energy produced at the inverter output would be calculated at 190.94 MWh, while using (31), the annual energy losses would be calculated at 2.748 MWh. Thus, the losses correspond to $2.748/190.94 = 0.0144$ or 1.44%. Thus, the combination of (31) and (13) give a reasonable evaluation of the losses in the ac cables with respect to the total energy produced at the inverter output, even during the design phase of the PV installation, where P_{max} is not known but it is estimated.

Since (26)–(29) and (32) were derived in a similar way as (31), we may say that they can be used for the accurate calculation of cable losses for the respective cases.

It is known that in grid-connected PV installations, the owner is paid only for the energy injected into the grid and not for the power. Using these equations, the design engineer can easily calculate the annual energy losses-and thus the annual income losses-for various r_{dc} and r_{ac}, that is, for various cable cross sections and lengths.

V. SELECTION OF THE OPTIMUM TRANSFORMER SIZE

The distribution network operator requires that a PV installation be connected in the medium voltage network (20 kV), through a step-up substation with one or more power transformers (20/0.4 kV), when the installed power is above a certain level, which is country-specific (for example, in Greece this level is 100 kW_p). It is known that the transformer losses consist of the core losses, which depend on the voltage level and the frequency, and the copper losses, which depend on the transformer loading. Thus, in a PV installation, the core losses are constant (assuming that the voltage level and frequency are constant) and appear during the whole year, that is, for 8760 h/yr. The copper losses vary with the square of the transformer current and appear for only $T_{max} = 4400$ h/yr.

Now, let us suppose that there are N_{tr} identical transformers, which are connected in parallel and inject the PV power into the medium-voltage grid. The total transformer losses at moment, t, are given by

$$P_{tr,loss}(t) = N_{tr} \cdot P_{Fe} + \frac{P_{Cu,N}}{N_{tr}} \left(\frac{S_i(t)}{S_N} \right)^2 \tag{33}$$

where P_{Fe} are the core losses and $P_{Cu,N}$ are the copper losses under the nominal operating power S_N of each identical transformer. $S_t(t)$ is the total apparent power loading of the installation at moment t. Given that a PV installation usually operates with unity power factor, the annual transformer energy losses are

$$E_{tr,loss} = \int_0^{T_y} P_{tr,loss}(t) \cdot dt = T_y \cdot N_{tr} \cdot P_{Fe} + \frac{P_{Cu,N}}{N_{tr} \cdot S_N^2} \int_0^{T_{max}} P_{dc}^2(t) dt \tag{34}$$

where T_y are the hours/yr for which the transformers are connected to the grid. Normally, $T_y = 8760$ h.

In case that $P_{inv,N} \geq P_{max}$, using (24) and (34), the annual energy losses become

$$E_{tr,loss} = T_y \cdot N_{tr} \cdot P_{Fe} + \frac{P_{Cu,N}}{N_{tr} \cdot S_N^2} W_1. \tag{35}$$

If $P_{inv,N} \leq P_{max}$, using (25) and (34), the annual energy losses become

$$E_{tr,loss} = T_y \cdot N_{tr} \cdot P_{Fe} + \frac{P_{Cu,N}}{N_{tr} \cdot S_N^2} W_2. \tag{36}$$

Equations (35) and (36) were derived under the assumption that the power at the transformer terminals is given by (3), that is, the losses in the inverters and ac cables were ignored. Although this approximation introduces an error, this error is insignificant for the following reasons: Firstly, it does not affect the selection of the optimum transformer size, as it will be shown later. Secondly, (35) and (36) should be used by the design engineer only in order to compare the annual energy losses between various transformer configurations rather than to estimate accurately the transformer losses for a given transformer configuration.

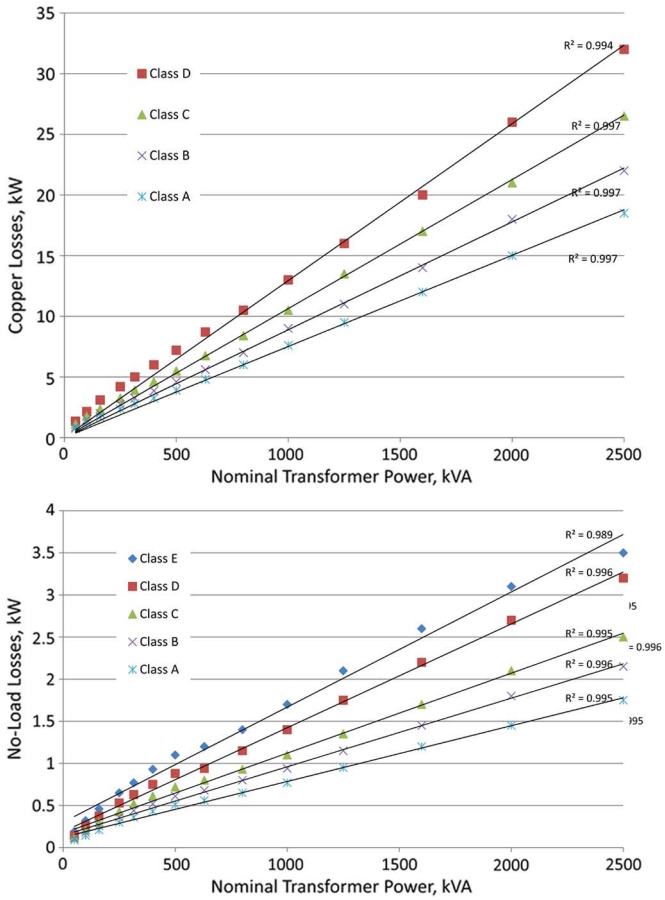

Fig. 7. Copper and core losses of oil-cooled distribution transformers according to the EN 50464 standard.

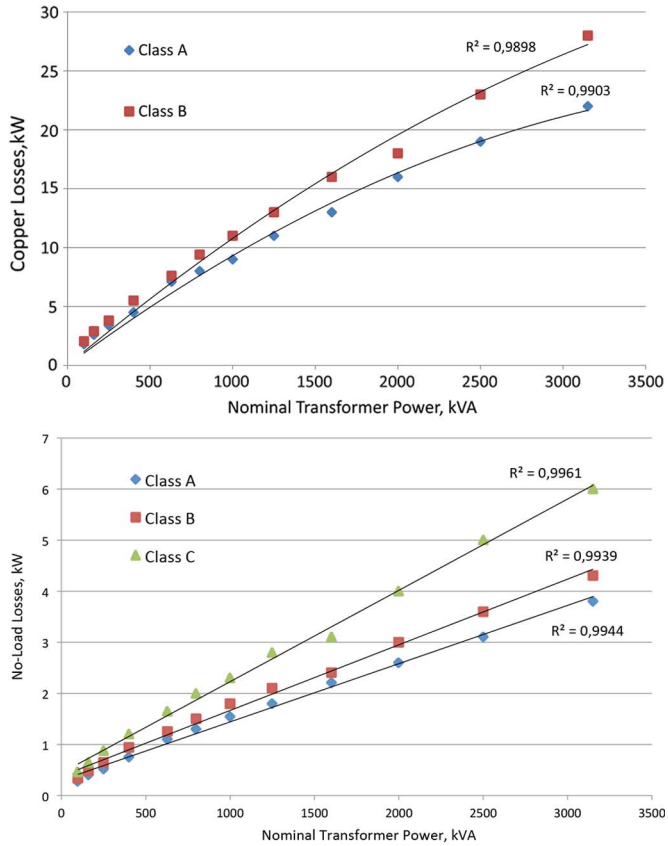

Fig. 8. Copper and core losses of the cast resin distribution transformers according to the EN 50541 standard.

The optimum transformer size (the size for which the annual losses are minimized) can be found from (35) or (36), if P_{Fe} and $P_{\mathrm{Cu,N}}$ are expressed in terms of S_{N}. There are generally two types of transformers used with PV Systems: oil-cooled and cast-resin transformers.

For oil-cooled distribution transformers, the EN 50464-1 standard [26] specifies five classes for the core losses (denoted as A_0, B_0, C_0, D_0 and E_0) and four classes for the copper losses (denoted as A_{k}, B_{k}, C_{k} and D_{k}). For cast-resin distribution transformers, the EN 50541-1 standard [27] specifies three classes for the no-load losses (denoted as A_0, B_0, and C_0) and two classes for the load losses (denoted as A_{k} and B_{k}).

Fig. 7(a) and (b) shows the oil-cooled transformer losses according to [26] for nominal power ratings in the range of 50–2500 kVA. It is evident from the linear correlation factors (R^2) shown in Fig. 7 that both loss types vary linearly with the transformer power rating. Thus, the oil-cooled transformer losses can be written as

$$P_{\mathrm{Fe}}(S_N) = l \cdot S_N + m \tag{37}$$

$$P_{\mathrm{Cu,N}}(S_N) = u \cdot S_N. \tag{38}$$

Respectively, Fig. 8(a) and (b) shows the cast-resin transformer losses according to [27] for nominal power ratings in the range of 100–3150 kVA. It is evident from the linear correlation factors (R^2), shown in Fig. 8, that the no-load losses vary linearly with the transformer power rating, while the load losses can be approximated with a second-order polynomial. Thus, the cast-resin transformer losses can be written as

$$P_{\mathrm{Fe}}(S_N) = n \cdot S_N + p \tag{39}$$

$$P_{\mathrm{Cu,N}}(S_N) = a \cdot S_N^2 + b \cdot S_N. \tag{40}$$

In case that $P_{\mathrm{inv,N}} \geq P_{\max}$, the optimum transformer size can be found if (37) and (38) for oil-cooled transformers or if (39) and (40) for cast-resin transformers are substituted in (35) and solve $(dE_{\mathrm{tr,loss}}/dS_N) = 0$ for S_{N}. Thus, we get

$$S_N^{\mathrm{opt}} = \frac{P_{\max}}{N_{\mathrm{tr}}} \cdot \sqrt{2 \cdot \frac{u}{l} \cdot \frac{T_{\max}}{T_y} \cdot [3 - 4 \cdot \ln(2)]} \tag{41}$$

for oil-cooled transformers and

$$S_N^{\mathrm{opt}} = \frac{P_{\max}}{N_{\mathrm{tr}}} \cdot \sqrt{2 \cdot \frac{b}{n} \cdot \frac{T_{\max}}{T_y} \cdot [3 - 4 \cdot \ln(2)]} \tag{42}$$

for cast-resin transformers.

If $P_{\mathrm{inv,N}} \leq P_{\max}$, the optimum transformer size can be found if (37) and (38) for oil-cooled transformers or if (39) and

TABLE VI
COEFFICIENTS OF (37) and (38) FOR VARIOUS LOSS CLASSES OF OIL-COOLED TRANSFORMERS

	l	m	u
Class A	$6.623\cdot10^{-4}$	0.123	$7.515\cdot10^{-3}$
Class B	$8.149\cdot10^{-4}$	0.145	$8.892\cdot10^{-3}$
Class C	$9.494\cdot10^{-4}$	0.173	$10.637\cdot10^{-3}$
Class D	$12.330\cdot10^{-4}$	0.190	$12.943\cdot10^{-3}$
Class E	$13.670\cdot10^{-4}$	0.301	

TABLE VII
COEFFICIENTS OF (39) and (40) FOR VARIOUS LOSS CLASSES OF CAST-RESIN TRANSFORMERS

	n	p	a	b
Class A	$1.14\cdot10^{-3}$	0.3014	$-1.131\cdot10^{-7}$	$1.044\cdot10^{-2}$
Class B	$1.285\cdot10^{-3}$	0.3811	$-9.893\cdot10^{-7}$	$1.176\cdot10^{-2}$
Class C	$1.788\cdot10^{-3}$	0.4411		

(40) for cast-resin transformers are substituted in (36) and solve $(dE_{\mathrm{tr,loss}}/dS_N) = 0$ for S_{N}. Thus, we obtain

$$S_N^{\mathrm{opt}} = \frac{P_{\max}}{N_{\mathrm{tr}}} \cdot \sqrt{8\cdot\frac{u}{l}\cdot\frac{T_{\max}}{T_y}\cdot\left[\ln\left(1-\frac{P_{\mathrm{inv,N}}}{2\cdot P_{\max}}\right)+\frac{P_{inv,N}}{2\cdot P_{\max}}\cdot\left(1+\frac{P_{\mathrm{inv,N}}}{2\cdot P_{\max}}\right)\right]} \quad (43)$$

for oil-cooled transformers and

$$S_N^{\mathrm{opt}} = \frac{P_{\max}}{N_{\mathrm{tr}}} \cdot \sqrt{8\cdot\frac{b}{n}\cdot\frac{T_{\max}}{T_y}\cdot\left[\ln\left(1-\frac{P_{inv,N}}{2\cdot P_{\max}}\right)+\frac{P_{inv,N}}{2\cdot P_{\max}}\cdot\left(1+\frac{P_{inv,N}}{2\cdot P_{\max}}\right)\right]} \quad (44)$$

for cast-resin transformers.

The l, m, and u parameters are given in Table VI for oil-cooled transformers, while for cast-resin transformers, the n, p, a, and b parameters are given in Table VII. P_{Fe} and $P_{\mathrm{Cu,N}}$ are in kilowatts provided that S_{N} is in kilovolt-amperes. It can be noticed from Tables VI and VII, for the same nominal power and class of losses, both the core and copper losses in cast-resin transformers are larger than the respective losses in oil-cooled transformers.

The accuracy of (41)–(44) in the calculation of the optimum transformer size was tested against detailed calculations for a hypothetical PV system of 200 $\mathrm{kW_p}$ (approximately) in each of the five locations (Fig. 2), for the cases where $P_{\mathrm{inv,N}} \leq P_{\max}$ and $P_{\mathrm{inv,N}} \geq P_{\max}$. The configuration of the various PV systems is shown in Table VIII.

If $P_{\mathrm{inv,N}} \leq P_{\max}$, the SMA 17-kW inverter type was selected whereas if $P_{\mathrm{inv,N}} \geq P_{\max}$, the Siemens 20-kW type was chosen. In each case, the same 240-$\mathrm{W_p}$ panel type, the same type of cables (dc: cross section $= 4\ \mathrm{mm^2}$, length $= 60$ m, ac: cross section $= 10\ \mathrm{mm^2}$, length $= 80$ m) were assumed. In the detailed calculations, the losses in the ac and dc cables and in the inverter were taken into account. A transformer with $\mathrm{A_0/B_k}$ loss class was assumed and by incrementally varying its nominal power, the optimum size was calculated based on the actual PDC.

TABLE VIII
CONFIGURATION OF APPROXIMATELY 200-kWp PV SYSTEM IN FIVE LOCATIONS

		No. of Inverters	strings/ inverter	panels/ string
Iraklion	$P_{\mathrm{inv,N}} \leq P_{\max}$	10	4	21
	$P_{\mathrm{inv,N}} \geq P_{\max}$	12	3	23
Madrid	$P_{\mathrm{inv,N}} \leq P_{\max}$	9	5	18
	$P_{\mathrm{inv,N}} \geq P_{\max}$	12	3	23
Munich	$P_{\mathrm{inv,N}} \leq P_{\max}$	6	6	23
	$P_{\mathrm{inv,N}} \geq P_{\max}$	8	5	21
Warsaw	$P_{\mathrm{inv,N}} \leq P_{\max}$	6	6	23
	$P_{\mathrm{inv,N}} \geq P_{\max}$	8	5	21
Edinburgh	$P_{\mathrm{inv,N}} \leq P_{\max}$	6	6	23
	$P_{\mathrm{inv,N}} \geq P_{\max}$	8	5	21

TABLE IX
ESTIMATION AND SELECTION OF OPTIMUM TRANSFORMER SIZE (IN KILOVOLT-AMPERES)—WHITE CELL: OIL-COOLED TRANSFORMERS. SHADED CELLS: CAST-RESIN TRANSFORMERS

	$P_{\mathrm{inv,N}} \leq P_{\max}$		$P_{\mathrm{inv,N}} \geq P_{\max}$		Selected size
	Calculation	(43)-(44)	Calculation	(41)-(42)	
Iraklion	311	320	311	319	315
	273	280	272	280	250 or 315
Madrid	301	287	311	297	250 or 315
	264	251	272	260	250
Munich	196	201	203	212	160 or 250
	172	176	178	186	160
Warsaw	183	195	189	202	160 or 250
	161	171	165	177	160
Edinburgh	171	189	174	193	160
	150	165	153	169	160

Table IX shows in comparison the optimum transformer size—for both oil-cooled and cast-resin types—calculated according to the detailed method and according to (41)–(44). The inaccuracies in Table IX are not significant, when the actual transformer size is to be selected, because transformers are built in certain kilovolt-amperes sizes (50, 100, 160, 250, etc.). Thus, the same transformer size will be selected either by using (41)–(44) or by detailed calculations. In this view, the accuracy of (41)–(44) is perfect.

As shown in Table IX, for the cases of Madrid, Munich, and Warsaw and for oil-cooled transformers, an engineer will have to choose a standardized transformer size that is either smaller or larger than the optimum one. The engineer could use (35) or (36) to compare the annual energy losses in the two transformers and then make their final selection, taking into account the transformer costs and the cost of the energy. For example, in the case of Munich, when $P_{\mathrm{inv,N}} \geq P_{\max}$, a 160-kVA transformer with $\mathrm{A_0/B_k}$ loss class will have-according to (35)-annual energy losses equal to 3640 kWh, while a 250-kVA transformer will have 3574 kWh. The difference of 66 kWh/annum in conjunction with the energy price can be compared with the price difference between the respective transformers. In the same way, using (35) or (36), a design engineer can compare transformers with not only different size but also different loss-class and type (cast-resin or oil-cooled). It can also be observed from Table IX that the optimum transformer size for the same location and

same class of losses is smaller for the cast-resin type than for the oil cooled one, because the losses of the cast-resin type are larger.

VI. Discussion and Conclusions

Analytical expressions for the PDC, inverter losses, inverter optimum size, dc and ac cable losses, transformer losses and optimum transformer size (for various loss classes) have been derived for PV systems on two-axis tracking systems in European locations.

It was shown that: 1) the PDC can be described by an expression, which requires only the maximum dc power as input. The maximum dc power can be easily found from the proper combinations of large solar irradiation and ambient temperature in summer months given in [22] for any European location; 2) the efficiency curve of any inverter can be described accurately by a simple mathematical expression with three unknown parameters [21]; and 3) the no-load and load losses of oil-cooled and cast-resin transformers vary with the transformer rating for a given class of losses, according to the EN 50464 and the EN 50541 standards. Thus, only the transformer rating, its type, and the loss class are required as input for the calculations.

The derived analytical expressions can be a very useful tool for the design engineers in order to compare the annual energy losses for various inverters, cables, and transformers in two-axis tracking PV systems of any size across Europe for given annual solar irradiation and ambient temperature conditions.

The accuracy and validity of the derived analytical expressions has been tested against detailed mathematical calculations and measurements. Due to the relatively stochastic nature of the solar irradiation and due to the assumptions and the simplifications introduced throughout this paper, the derived expressions should not be used for the calculation of the absolute energy yields or energy losses, but for comparing energy yields and energy losses between different inverters, cables, and transformers for given climate data.

References

[1] F. Trieb, O. Langnib, and H. Klaiss, "Solar electricity generation-a comparative view of technologies, costs and environmental impact," *Solar Energy*, vol. 59, no. 1–3, pp. 89–99, Jan. 1997.

[2] N. H. Helwa, A. B. G. Bahgat, and A. M. , "Computation of the solar energy captured by different solar tracking systems," *Energy Sources*, vol. 22, no. 1, pp. 35–44, Jan. 2000.

[3] N. H. Helwa, A. B. G. Bahgat, and A. M. , "Maximum collectable solar energy by different solar tracking systems," *Energy Sources*, vol. 22, no. 1, pp. 23–34, Jan. 2000.

[4] J. Monedero, F. Dobon, A. Lugo, P. Valeraz, R. Osunaz, L. Acosta, and G. N. Marichal, "Minimizing energy shadow losses for large PV plants," presented at the 3rd World Conf. Photovoltaic Energy Convers., Osaka, Japan, May 11–18, 2003.

[5] S. Abdallah, "The effect of using sun tracking systems on the voltage—Current characteristics and power generation of flat plate photovoltaics," *Energy Convers. Manage.*, vol. 45, no. 11–12, pp. 1671–1679, Jul. 2004.

[6] S. Abdallah and S. Nijmeh, "Two axes sun tracking system with PLC control," *Energy Convers. Manage.*, vol. 45, no. 1, pp. 1931–1939, Jul. 2004.

[7] T. Huld, M. Suri, and E. D. Dunlop, "Comparison of potential solar electricity output from fixed-inclined and two-axis tracking photovoltaic modules in Europe," *Prog. Photovolt. Res. Appl.*, vol. 16, no. 1, pp. 47–59, Jan. 2008.

[8] L. Narvarte and E. Lorenzo, "Tracking and ground cover ratio," *Prog. Photovolt. Res. Appl.*, vol. 16, no. 98, pp. 703–714, Dec. 2008.

[9] H. Mousazadeh, A. Keyhania, A. Javadi, H. Mobli, K. Abrinia, and A. Sharifi, "A review of principle and sun-tracking methods for maximizing solar systems output," *Renew. Sustain. Energy Rev.*, vol. 13, no. 8, pp. 1800–1818, Oct. 2009.

[10] C.-Y. Lee, P.-C. Chou, C.-M. Chiang, and C.-F. Lin, "Sun tracking systems: A review," *Sensors*, vol. 9, no. 5, pp. 3875–3890, May 2009.

[11] R. Eke and A. Senturk, "Performance comparison of a double-axis sun tracking versus fixed PV system," *Solar Energy*, vol. 86, no. 9, pp. 2665–2672, Sep. 2012.

[12] H. Riess and P. Sprau, "Design considerations for the PV generator/inverter matching in grid connected systems," in *Proc. 11th Eur. Photovoltaic Solar Energy Conf.*, Montreux, Switzerland, 1992, pp. 1377–1378.

[13] K. Peippo and P. D. Lund, "Optimal sizing of grid-connected PV-systems for different climates and array orientations: A simulation study," *Solar Energy Mater. Solar Cells*, vol. 35, pp. 445–451, Sep. 1994.

[14] L. Keller and P. Affolter, "Optimizing the panel area of a photovoltaic system in relation to the static inverter-practical results," *Solar Energy*, vol. 55, no. 1, pp. 1–7, Jul. 1995.

[15] A. E.-M. M. Abd El-Aal, J. Schmid, J. Bard, and P. Caselitz, "Modeling and optimizing the size of the power conditioning unit for photovoltaic systems," *J. Sol. Energy Eng.*, vol. 128, no. 1, pp. 40–44, 2006.

[16] J. D. Mondol, Y. G. Yohanis, and B. Norton, "Optimal sizing of array and inverter for grid-connected photovoltaic systems," *Solar Energy*, vol. 80, no. 12, pp. 1517–1539, Dec. 2006.

[17] A. Kornelakis and E. Koutroulis, "Methodology for the design optimisation and the economic analysis of grid-connected photovoltaic systems," *IET Renew. Power Gen.*, vol. 3, no. 4, pp. 476–492, Dec. 2009.

[18] J. Muñoz, F. Martinez-Moreno, and E. Lorenzo, "On-site characterisation and energy efficiency of grid-connected PV inverters," *Prog. Photovolt. Res. Appl.*, vol. 19, no. 2, pp. 192–201, Mar. 2011.

[19] T. Khatib, A. Mohamed, and K. Sopian, "A review of photovoltaic systems size optimization techniques," *Renew. Sustain. Energy Rev.*, vol. 22, pp. 454–465, Jun. 2013.

[20] S. Chen, P. Li, D. Brady, and B. Lehman, "Determining the optimum grid-connected photovoltaic inverter size," *Solar Energy*, vol. 87, pp. 96–116, Jan. 2013.

[21] C. Demoulias, "A new simple analytical method for calculating the optimum inverter size in grid-connected PV plants," *Elect. Power Syst. Res.*, vol. 80, no. 10, pp. 1197–1204, Oct. 2010.

[22] PVGIS, Free online estimation of the solar irradiance and ambient temperature in any European and African location. 2001–2012. [Online]. Available: http://re.jrc.ec.europa.eu/pvgis/apps4/pvest.php

[23] S. Krauter, *Solar Elect. Power Gen.-Photovolt. Energy Syst.*. Berlin, Germany: Springer-Verlag, 2006, pp. 28–37.

[24] *Procedures for Temperature and Irradiance Corrections to Measured I—V Characteristics of Crystalline Silicon Photovoltaic (PV) Devices*, IEC Standard 60891, 1992.

[25] *Planning and Installing Photovoltaic Systems: A Guide for Installers, Architects and Engineers*, 2nd ed. London, U.K.: Earthscan, 2008, pp. 111–112, Deutsche Gesellschaft für Sonnenenergie.

[26] *Three-Phase Oil-Immersed Distribution Transformers 50 Hz, From 50 kVA to 2500 kVA With Highest Voltage for Equipment Not Exceeding 36 kV-Part 1: General Requirements*, EN Standard 50464-1, 2007.

[27] *Three-Phase Dry-Type Distribution Transformers 50 Hz, From 100 kVA to 3150 kVA With Highest Voltage for Equipment Not Exceeding 36 kV-Part 1: General Requirements*, EN Standard 50541-1, 2009.

Kyriaki-Nefeli D. Malamaki was born in 1986. She received the Diploma in electrical and computer engineering from the Aristotle University of Thessaloniki, Thessaloniki, Greece, in 2012, where she is currently pursuing the Ph.D. degree in electrical and computer engineering.

Her research interests are in the fields of power quality, and the interface of renewable energy sources with the grid and power-electronic converters.

Charis S. Demoulias (M'96–SM'11) was born in 1961. He received the Diploma and Ph.D. degrees in electrical engineering from the Aristotle University of Thessaloniki, Thessaloniki, Greece, in 1984 and 1991, respectively.

Currently, he is Assistant Professor with the Electrical Machines Laboratory, Department of Electrical and Computer Engineering, Aristotle University of Thessaloniki. His research interests are in the fields of power electronics, harmonics, electric motion systems, and renewable energy sources.